ACS APPLIED MATERIALS & INTERFACES

RESEARCH ARTICLE

www.acsami.org

One-Step Ge/Si Epitaxial Growth

Hung-Chi Wu,[†] Bi-Hsuan Lin,[‡] Huang-Chin Chen,[§,⊥] Po-Chin Chen,[†] Hwo-Shuenn Sheu,[‡] I-Nan Lin,[§] Hsin-Tien Chiu,[#] and Chi-Young Lee[*,⊥]

[†]Department of Materials Science and Engineering and [⊥]Center for Nanotechnology, Materials Science, and Microsystems National Tsing Hua University, Hsinchu, Taiwan 30013, Republic of China

[‡]Research Division, National Synchrotron Radiation Research Center, Hsinchu, Taiwan 30076, Republic of China

[§]Department of Physics, Tamkang University, Tamsui, Taiwan 25137, Republic of China

[#]Department of Applied Chemistry, National Chiao Tung University, Hsinchu, Taiwan 30010, Republic of China

Supporting Information

ABSTRACT: Fabricating a low-cost virtual germanium (Ge) template by epitaxial growth of Ge films on silicon wafer with a Ge_xSi_{1-x} ($0 < x < 1$) graded buffer layer was demonstrated through a facile chemical vapor deposition method in one step by decomposing a hazardousless GeO_2 powder under hydrogen atmosphere without ultra-high vacuum condition and then depositing in a low-temperature region. X-ray diffraction analysis shows that the Ge film with an epitaxial relationship is along the in-plane direction of Si. The successful growth of epitaxial Ge films on Si substrate demonstrates the feasibility of integrating various functional devices on the Ge/Si substrates.

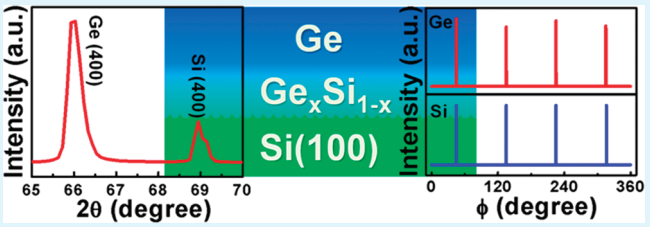

KEYWORDS: germanium (Ge), silicon (Si), epitaxial growth, chemical vapor deposition (CVD), one-step growth

1. INTRODUCTION

Germanium (Ge) has attracted much attention because of its several superior intrinsic properties towards silicon (Si), such as large excitonic Bohr radius (Ge: 24.3 nm; Si: 4.9 nm), high carrier mobility (Ge has 2.75 times increase in bulk electron and 4 times increase in hole mobility than Si), and small energy bandgap (direct and indirect bandgap for Ge are 0.8 and 0.66 eV, and for Si are 3.2 and 1.12 eV); furthermore, Ge has a strong absorption band at near-infrared wavelength and high refractive index.[1−3] These advantageous properties of Ge lead to an alternative semiconductor material for its potential use in electronic and optoelectronic applications.[4−10] Along with the progressive miniaturization of Si-based electronics, current small-sized electronic platforms meet a significant problem while attempting to match up with the constantly increasing requirements for higher speed and throughput.[11,12] Consequently, the integration of a high-quality Ge layers on Si enhances device performances and helps to continue traditional silicon scaling which motivates numerous researches in the recent years. High-quality Ge on Si continues to remain technologically important for several notable applications.[4−10]

Although Ge has better advantageous properties than Si and may be included into the Si-based transistor scaling path, the practical use of bulk Ge for semiconductor industry still meets several problems, especially the lattice mismatch (4.17%) between Ge and Si.[13−17] The large lattice mismatch would lead to the relaxed epitaxial Ge film growth on Si substrate dominating by islanding and misfit dislocations, and therefore a thick Ge_xSi_{1-x} ($0 < x < 1$) buffer layer is formed.[14−17] For further applications to be studied, deterministic control of orientation and crystal structure is necessary. As a result, it is important to overcome the mismatch and to grow high quality crystalline Ge epilayers on Si substrate that are much suitable for Si-based transistor integration.

Various approaches have been used to grow epitaxial Ge films, including chemical vapor deposition (CVD),[18,19] ion beam sputter deposition,[20] a solution method coupled with annealing,[21] and several epitaxial growth methods, such as molecular beam epitaxy (MBE),[16,22] chemical beam epitaxy,[23] solid-phase (or surfactant-mediated) epitaxy.[24,25] So far, CVD and MBE have been mainly employed to fabricate Ge films on Si for producing Ge/Si heterodevices. However, both methods are operating under an ultra-high vacuum (UHV) atmosphere, and the growth rate of MBE is too slow for mass production. On the contrary, CVD offers many advantages, such as high throughput, in situ doping and selective deposition, yet hazardous germane (GeH_4) and its derivatives have been widely utilized as Ge precursors in CVD to prepare Ge films.[18,19] Therefore, finding a hazardousless and environment-friendly Ge precursor is necessary.

In this work, a wafer-scaled Ge layer with Ge_xSi_{1-x} buffer layer was epitaxially grown on a Si substrate in one step process via a facile CVD method without UHV condition by thermal decomposition of a safe precursor, germanium(IV) oxide (GeO_2), under a hydrogen (H_2) atmosphere.

Received: March 12, 2011
Accepted: May 31, 2011
Published: June 08, 2011

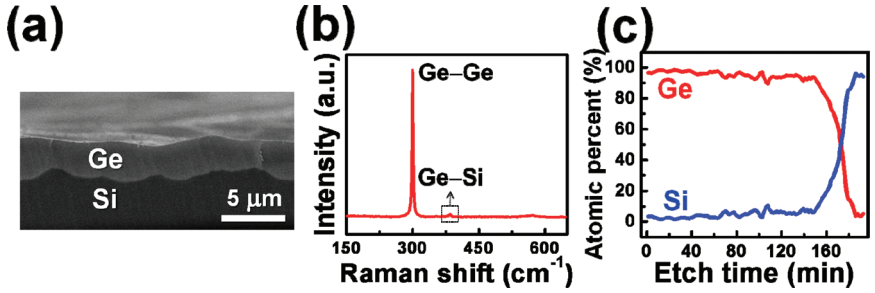

Figure 1. (a) Cross-sectional SEM image of the silver-gray film on silicon substrate. (b) Raman spectrum for the as-grown film on silicon substrate; (c) Auger depth analysis for the as-grown film with the thickness of about 5 μm grown on Si substrate, and the as-grown film has 4 μm high purity Ge layer on a 1 μm gradient Ge_xSi_{1-x} layer.

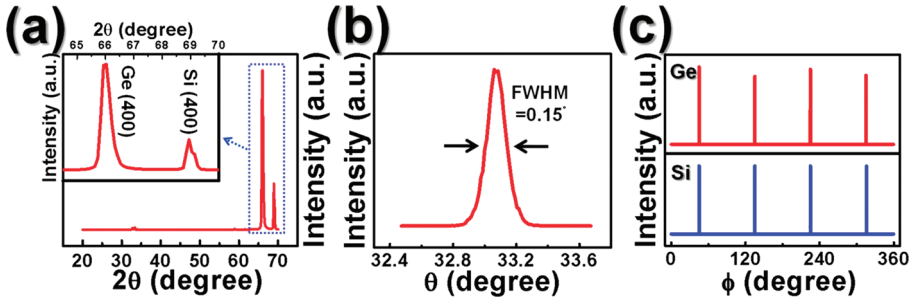

Figure 2. (a) XRD $\theta-2\theta$ scan profile of the as-grown Ge film on Si(100) substrate, the range of 65−70° was magnified and shown in the inset; (b) rocking curve of the Ge(400) reflection; (c) XRD φ scan profiles for the off-normal (111) plane of the Ge film and Si(111).

2. EXPERIMENTAL SECTION

A. Synthesis. The Ge film was obtained by CVD method[26] in a horizontal hot-wall quartz tube reactor comprised of a pumping system and a reaction chamber heated by a tubular furnace. After RCA cleaning steps, cleaned Si wafers with [100] orientation were used as the substrates. The highly pure GeO_2 powder was used as the source material placed in an alumina boat in the high-temperature zone and the cleaned substrates were placed in the low temperature zone to downstream of the reaction chamber. Before heating, the reaction chamber was pumped to a vacuum pressure of 10^{-3} Torr. Then, the carrier gas, H_2, was introduced into the reaction chamber at a flow rate of 90 sccm (standard cubic centimeters per minute). The temperature was set as 1100 °C in the high-temperature zone with chamber pressure maintained about 15−20 Torr for different durations (1.5, 3, and 6 h).

B. Characterization. The as-synthesized samples were studied by X-ray diffraction (Bruker D8) using Cu K_α radiation, and φ scan measurements were performed with a four-circle diffractometer (Huber, D-8219 Rimsting). The micro-Raman system (Lab Raman HR800, Jobin Yvon) was using a He−Ne laser with a wavelength of 632.8 nm. The surface morphology and crystallinity of the as-synthesized samples were observed under a scanning electron microscope (SEM, JEOL−6500F) and a transmission electron microscope (TEM, JEOL−2100F), respectively. The chemical compositions of the products were analyzed by energy-dispersive spectroscopy (EDS) that is equipped on SEM and TEM. The Auger depth profile was obtained on a VG Scientific Microlab 350.

3. RESULTS AND DISCUSSION

A silver-gray film was obtained on the Si (100) substrate at the downstream region of the thermal CVD in one step process by using GeO_2 powder as a precursor under H_2 atmosphere in a tubular furnace. The coverage of this silver-gray film was about 16 cm, corresponding to a temperature range of 1000−920 °C, and the SEM/EDS analysis indicates the composition of this silver-gray film was only Ge. From the cross-sectional SEM investigation, the thickness of this film gradually decreased from 10 μm to 0.2 μm from upstream to downstream side. In addition to that, the cross-sectional SEM image shown in Figure 1a shows an undulated interface between Ge film and Si substrate. Further, the Ge film grown on Si(100) substrate was identified by a micro-Raman system shown in Figure 1b. A sharp peak appeared at around 300 cm^{-1} is consistent with a Ge−Ge bond stretching vibration; in addition, a very weak peak appeared at 390 cm^{-1} could be assigned to Ge−Si bond stretching.[27] Further, Auger depth analysis of the Ge film grown on Si substrate indicated that the film grown on Si substrate contained several micrometer high purity Ge layer on a gradient Ge_xSi_{1-x} ($0 < x < 1$) layer shown in Figure 1c.

Further, the structural properties of the Ge film were characterized by XRD. Figure 2a shows the typical $\theta-2\theta$ scan XRD profile of the Ge film deposited on Si(100) substrate. Two sharp peaks appeared at around $2\theta = 69$ and 66° were assigned to the (400) planes of the Si(100) substrate (JCPDS card no. 75-0589) and (400) planes of cubic Ge (JCPDS card no. 89-2768), respectively. Usually, the singular sharp XRD signal crystal resulted from the superiorly preferred orientation growth. Therefore, the normal of the Ge film has a [100] orientation parallels to the [100] of the underneath Si(100) substrate. In addition, the full width at half maximum (FWHM) value of the (400) rocking curve of Ge is 0.15° (Figure 2b, a FWHM value of the (400) rocking curve for Si substrate is 0.03°), which strongly supports the good crystalline quality of the Ge layer. The growth direction of the germanium film was further studied by φ scan profile, as shown in Figure 2c. The φ scan profile for the off-normal (111)

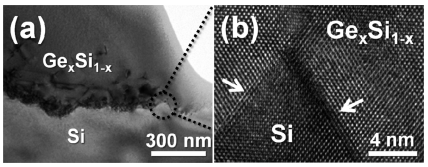

Figure 3. Interface between the as-grown film and silicon substrate: (a) typical TEM image; (b) HR-TEM image form the circled region in (a).

planes of the Ge film shows a four-fold azimuthal symmetry superposed that of Si(100) substrate indicates the in-plane orientation of the Ge film and parallels to silicon substrate. Based on these XRD results indicate that the silver-gray Ge film epitaxially grew on Si(100) substrate through the simple CVD method in one step. Further experiments were carried out by using Si(110) and Si(111) as substrates, and the resulting Ge films also show an epitaxial behavior as shown in Figure S1 in the Supporting Information.

In addition, Figure 3a represents the cross-sectional TEM investigation from the interface between the grown thin film and Si substrate. The dislocation induced contrast is visible at the interface. Further, Figure 3b shows a high-resolution TEM image from the circled region in Figure 3a, the dislocations were clearly indicated as arrows. TEM/EDS elemental line profiles (Figure S2 in the Supporting Information) of the as-grown film on silicon substrate shows a gradient change from the buffer Ge_xSi_{1-x} layer.

Moreover, the Ge epilayers grown on Si substrate for different deposition time were observed by SEM (Figure S3 in the Supporting Information). When the growth time was 1.5 h, many holes formed on the silicon surface, whereas when the growth time increased to 3 h, some of the holes were filled up by germanium, and many islands formed on surface instead. As the growth time was prolonged to 6 h, the Ge film get thicker and the islands become larger. Based on the above investigations, the fundamental growth route was suggested as follows: GeO_2 (melting point: 1086 °C) was initially reduced by H_2 in the high temperature regions (1100 °C) to form Ge, GeO_y ($0 < y < 2$) and H_2O, and then subsequently flowed to the lower temperature region to react with the silicon substrate. H_2O and GeO_y could be the etching reagent resulting for holes formation, whereas Ge causes the deposition. Moreover, while surface silicons were oxidized by GeO_y, Ge (in GeO_y) would take the place of Si, resulting in the formation of Ge layers on silicon. Ge_xSi_{1-x} graded layer formed for the accommodation of the large lattice mismatch between Si and Ge,[15−17] Following the Ge layer formed above the buffer layer by precipitating Ge which was formed by reaction of GeO_2 and H_2. The dislocations appeared at the interface between Ge_xSi_{1-x} layer and Si substrate may account for the mismatch induced stress relieving by dislocation networks (Figure 3a).

4. CONCLUSION

In summary, a virtual Ge template composed of Ge epilayer with a Ge_xSi_{1-x} buffer layer on Si substrate can be obtained in one step process via CVD method without UHV condition by a thermal decomposition of a hazardousless GeO_2 powder under a H_2 atmosphere. Structural analyses show high-crystallinity films with preferential orientation and thickness up to several micrometers could be produced. The successful growth of epitaxial Ge films on Si demonstrates the feasibility of integrating various functional devices on the Ge/Si templates.

■ ASSOCIATED CONTENT

Supporting Information. Figure S1, XRD $\theta-2\theta$ scan profiles of Ge films grew on Si(110), and Si(111) substrates; Figure S2, TEM and EDS elemental line profiles of the as-grown film on silicon substrate; Figure S3, Ge epilayers grown on Si substrate for different deposition time. This material is available free of charge via the Internet at http://pubs.acs.org.

■ AUTHOR INFORMATION

Corresponding Author
*E-mail: cylee@mx.nthu.edu.tw.

■ ACKNOWLEDGMENT

The authors thank Miss Shalini Jayakumar for grammatical editing, Miss Ting-Hsun Chang for the experimental help, and the National Science Council of the Republic of China, Taiwan, for financially supporting this research under Contract NSC-96-2113-M-007-021-MY3, NSC-97-2113-M-009-015-MY3, and NSC-99-2113-M-007-011.

■ REFERENCES

(1) Streetman, B.; Banerjee, S. *Solid State Electronic Devices*, 6th ed.; Prentice Hall: Upper Saddle River, NJ, 2005.
(2) Sze, S. M.; Ng, K. K. *Physics of Semiconductor Devices*, 3rd ed.; Wiley: New York, 2007.
(3) Colace, L.; Masini, G.; Assanto, G. *IEEE J. Quantum Electron.* **1999**, *35*, 1843–1852.
(4) Nayfeh, A.; Chui, C. O.; Yonehara, T.; Saraswat, K. C. *IEEE Electron. Device Lett.* **2005**, *26*, 311–313.
(5) Dey, S.; Joshi, S.; Garcia-Gutierrez, D.; Chaumont, M.; Campion, A.; Jose-Yacaman, M.; Banerjee, S. K. *J. Electron Mater.* **2006**, *35*, 1607–1612.
(6) Lubyshev, D.; Fastenau, J. M.; Wu, Y.; Liu, W. K.; Bulsara, M. T.; Fitzgerald, E. A.; Hoke, W. E. *J. Vac. Sci. Technol., B* **2008**, *26*, 1115–1119.
(7) Feng, D. Z.; Liao, S. R.; Dong, P.; Feng, N. N.; Liang, H.; Zheng, D. W.; Kung, C. C.; Fong, J.; Shafiiha, R.; Cunningham, J.; Krishnamoorthy, A. V.; Asghari, M. *Appl. Phys. Lett.* **2009**, *95*, 261105.
(8) Luan, H. C.; Wada, K.; Kimerling, L. C.; Masini, G.; Colace, L.; Assanto, G. *Opt. Mater.* **2001**, *17*, 71–73.
(9) Leonhardt, D.; Sheng, J.; Cederberg, J. G.; Li, Q. M.; Carroll, M. S.; Han, S. M. *Thin Solid Films* **2010**, *518*, 5920–5927.
(10) Beeler, R.; Mathews, J.; Weng, C.; Tolle, J.; Roucka, R.; Chizmeshya, A. V. G.; Juday, R.; Bagchi, S.; Menendez, J.; Kouvetakis, J. *Sol. Energ. Mat. Sol. C* **2010**, *94*, 2362–2370.
(11) Theis, T. N.; Solomon, P. M. *Science* **2010**, *327*, 1600–1601.
(12) Lundstrom, M. *Science* **2003**, *299*, 210–211.
(13) Silvestri, H. H.; Bracht, H.; Hansen, J. L.; Larsen, A. N.; Haller, E. E. *Semicond. Sci. Technol.* **2006**, *21*, 758–762.
(14) Bean, J. C. *Science* **1985**, *230*, 127–131.
(15) Samavedam, S. B.; Fitzgerald, E. A. *J. Appl. Phys.* **1997**, *81*, 3108–3116.
(16) Herman, M. A. *Cryst. Res. Technol.* **1999**, *34*, 583–595.
(17) Kahng, S. J.; Ha, Y. H.; Moon, D. W.; Kuk, Y. *J. Vac. Sci. Technol., A* **2000**, *18*, 1937–1940.
(18) Mukherjee, C.; Seitz, H.; Schroder, B. *Appl. Phys. Lett.* **2001**, *78*, 3457–3459.
(19) Kobayashi, S.; Cheng, M. L.; Kohlhase, A.; Sato, T.; Murota, J.; Mikoshoba, N. *J. Cryst. Grwoth* **1990**, *99*, 259–262.
(20) Tomasch, G. A.; Kim, Y. W.; Markert, L. C.; Lee, N. E.; Greene, J. E. *Thin Solid Films* **1993**, *223*, 212–217.
(21) Zou, G. F.; Luo, H. M.; Ronning, F.; Sun, B. Q.; McCleskey, T. M.; Burrell, A. K.; Bauer, E.; Jia, Q. X. *Angew. Chem. Int. Ed.* **2010**, *49*, 1782–1785.

(22) Liu, J.; Kim, H. J.; Hul'ko, O.; Xie, Y. H.; Sahni, S.; Bandaru, P.; Yablonovitch, E. *J. Appl. Phys.* **2004**, *96*, 916–918.
(23) Eres, D.; Lowndes, D. H.; Tischler, J. Z. *Appl. Phys. Lett.* **1989**, *55*, 1008–1010.
(24) Lu, G. Q.; Nygren, E.; Aziz, M. J.; Turnbull, D.; White, C. W. *Appl. Phys. Lett.* **1990**, *56*, 137–139.
(25) Wietler, T. F.; Bugiel, E.; Hofmann, K. R. *Thin Solid Films* **2006**, *508*, 6–9.
(26) Wu, H. C.; Hou, T. C.; Chueh, Y. L.; Chen, L. J.; Chiu, H. T.; Lee, C. Y. *Nanotechnology* **2010**, *21*, 455601.
(27) Baranov, A. V.; Fedorov, A. V.; Perova, T. S.; Moore, R. A.; Solosin, S.; Yam, V.; Bouchier, D.; Thanh, V. L. *J. Appl. Phys.* **2004**, *96*, 2857–2863.